Nonisothermal Crystallization Kinetics of Low-Density Polyethylene Inside Percolating Network of ZnO Nanoparticles

Guo-Dong Liang,[1,2] Wang-Ping Qin,[1] Ting-Ting Liu,[1] Fang-Ming Zhu,[1,2] Qing Wu[1,2]

[1]*DSAPM Lab, Institute of Polymer Science, School of Chemistry and Chemical Engineering, Sun Yat-Sen University, Guangzhou 510275, People's Republic of China*
[2]*PCFM Lab of CM Institute, Sun Yat-Sen University, Guangzhou 510275, People's Republic of China*

Received 29 July 2011; accepted 29 September 2011
DOI 10.1002/app.36341
Published online 27 December 2011 in Wiley Online Library (wileyonlinelibrary.com).

ABSTRACT: The nonisothermal crystallization of low-density polyethylene inside percolating network of ZnO nanoparticles (LDPE/60 vol % ZnO) was investigated via differential scanning calorimetry (DSC), and compared to that of LDPE bulk (pristine LDPE and LDPE/1.15 vol % ZnO). The results revealed that crystallization behavior of LDPE inside ZnO percolating network was quite different from that of LDPE bulk. The former showed $\sim 4^{\circ}C$ higher crystallization onset temperatures contrasting to the latter, demonstrating nucleation effect of ZnO on LDPE crystallization. On the other hand, much longer half-crystallization times were observed for the former, illustrating that crystallization of LDPE is retarded by the continuous ZnO network to some extent. Moreover, LDPE embedded inside ZnO network has by far larger crystallization activation energy and smaller specific free energy of the folding surface in contrast to LDPE bulk. Finally, nonisothermal crystallization kinetics study illustrated that both modified Avrami and Liu methods could be used to describe satisfactorily nonisothermal crystallization kinetics for all the samples investigated. © 2011 Wiley Periodicals, Inc. J Appl Polym Sci 125: E113–E121, 2012

Key words: composites; crystallization; nanoparticles; polyethylene

INTRODUCTION

Investigation of crystallization behavior of crystalline polymers is of great importance from both academic and technological aspects as physical properties and mechanical performances of crystalline polymers are strongly dependent on their crystalline structures, which are dictated with crystallization kinetics.[1–8] Crystallization of polymers can be investigated by means of isothermal and nonisothermal studies. As most of fabrication processes for polymeric materials such as injection and extrusion molding are conducted under nonisothermal condition, investigation of nonisothermal crystallization behavior is of pronounced significance from technological viewpoint. Moreover, in contrast to isothermal crystallization, nonisothermal crystallization is carried out over broad temperature range, which allows understanding the overall crystallization behavior during solidification of polymers. Up to now, researchers have developed theoretical and experimental approaches for investigating nonisothermal crystallization behavior of polymers, and nonisothermal study has become an important tool to optimize the operating condition in polymer processing.[9–11]

Polymer composites consisting of inorganic fillers and polymeric matrices are regarded as a catalogue of promising materials due to cost-efficiency, superior mechanical properties, excellent chemical resistance, and so on.[12–23] The filler particles are uniformly dispersed assumedly through polymer matrix at low filler loading. As increasing filler content, filler particles begin to link together to form clusters. Further increasing filler content leads to the formation of infinite network of filler particles. Such geometric phase transition from isolated filler particles into interconnected infinite network is referred as percolation transition, which is accompanied with a sharp change in physical properties such as electrical resistivity.[24] In a percolating system, filler particles form continuous phase and polymers are located inside interconnected filler network.

Nonisothermal crystallization behavior of crystalline polymers reinforced with inorganic fillers has been widely investigated so far.[25–34] In the presence of fillers with high surface energy and aspect ratio, crystallization of polymers is pronouncedly expedited as the fillers tend to absorb polymer segments

Correspondence to: G.-D. Liang (lgdong@mail.sysu.edu.cn).

Contract grant sponsor: National Natural Science Foundation of China; contract grant number: 21074151.

to induce nuclei formation upon crystallization. Most of studies focused on the polymeric composites at low filler loading where filler particles were distributed in continuous polymers matrices. However, crystallization behavior of crystalline polymers inside percolating systems is rarely reported. In such a system, polymer segments are restrained inside percolating network. Both nuclei formation and crystal growth that dominate crystallization kinetics are affected by the geometric confinements. As a result, totally different crystallization behavior is anticipated in contrast to polymer bulk.

In a previous work,[35,36] we found that as ZnO content approached 52 vol %, ZnO particles began to connect each other to form percolating network, which provides a novel surrounding for investigating crystallization behavior of polymers under confinements. In the present work, we report the nonisothermal crystallization kinetics of low-density polyethylene (LDPE) embedded inside the percolating network of ZnO nanoparticles. The results reveal that crystallization behavior of the LDPE inside ZnO network is noticeably different contrasting with LDPE bulk.

EXPERIMENTAL

Preparation

LDPE/ZnO nanocomposites were prepared by melt compounding commercial LDPE pellets (LDPE, M_w = 50,000 g/mol) with ZnO particles in a Brabender mixer. ZnO nanoparticles of $\sim$ 200 nm were supplied by Nanostructrued and Amorphous Materials. To avoid thermal degradation of the polymer matrix, the mixing time was set to 15 min at 180°C.

Scanning electron microscopy

Morphologies of LDPE/1.15 vol % ZnO and LDPE/60 vol % ZnO composites were examined with a JEOL JSM 820 SEM. The specimens were fractured with a hammer in liquid nitrogen, followed by drying at 40°C under reduced pressure overnight and coated with a thin gold layer before SEM observation.

Differential scanning calorimetry

Nonisothermal crystallization behavior of LDPE/ZnO nanocomposites was investigated with a TA Instruments differential scanning calorimetry (DSC) (model 2910) under nitrogen atmosphere. Temperature was calibrated with indium before testing. The LDPE/ZnO nanocomposites (about 5 mg) were sealed in aluminum pans. The samples were held at 180°C for 5 min to eliminate previous thermal history and cooled to room temperature at the prescribed rates (such as 2, 5, 10, and 20°C min^{-1}), followed by heating to 180°C at a rate of 10°C min^{-1}.

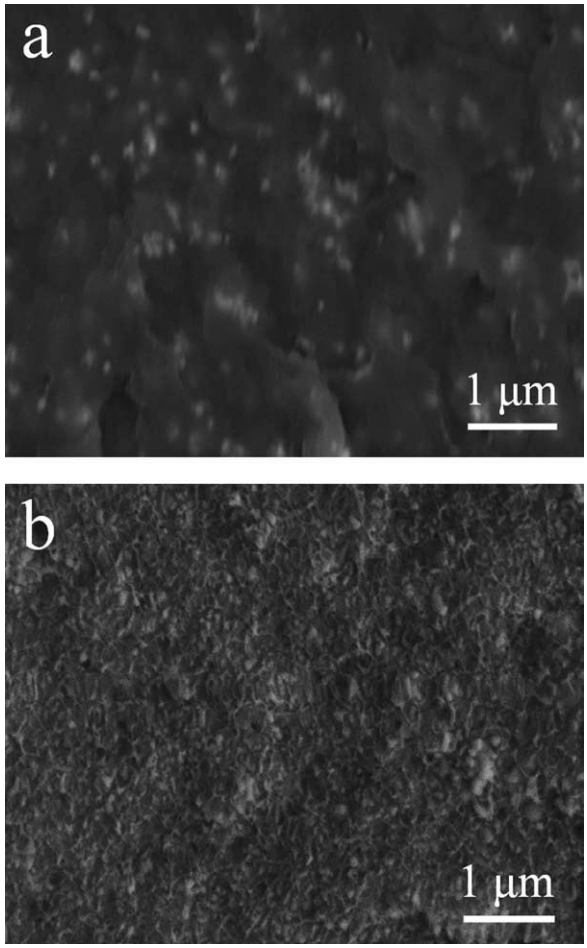

Figure 1 SEM images of LDPE/1.15 vol % ZnO (a) and LDPE/60 vol % ZnO (b).

RESULTS AND DISCUSSION

Morphology

Figure 1 shows SEM images of LDPE/ZnO composites. ZnO particles are recognized as bright dots in SEM images. It is obvious that fracture surface embedded with separate ZnO particles (or clusters) is observed for LDPE/1.15 vol % ZnO. While LDPE/60 vol % ZnO exhibits much rough fracture surface consisting of concaves formed by pulling out of ZnO nanoparticles. Such impacted concaves implies that ZnO particles are closely packed in LDPE/60 vol % ZnO and that LDPE is embedded inside ZnO network.[35,36]

Crystallization behavior

Figure 2 shows the nonisothermal crystallization DSC traces of LDPE/60 vol % ZnO at various

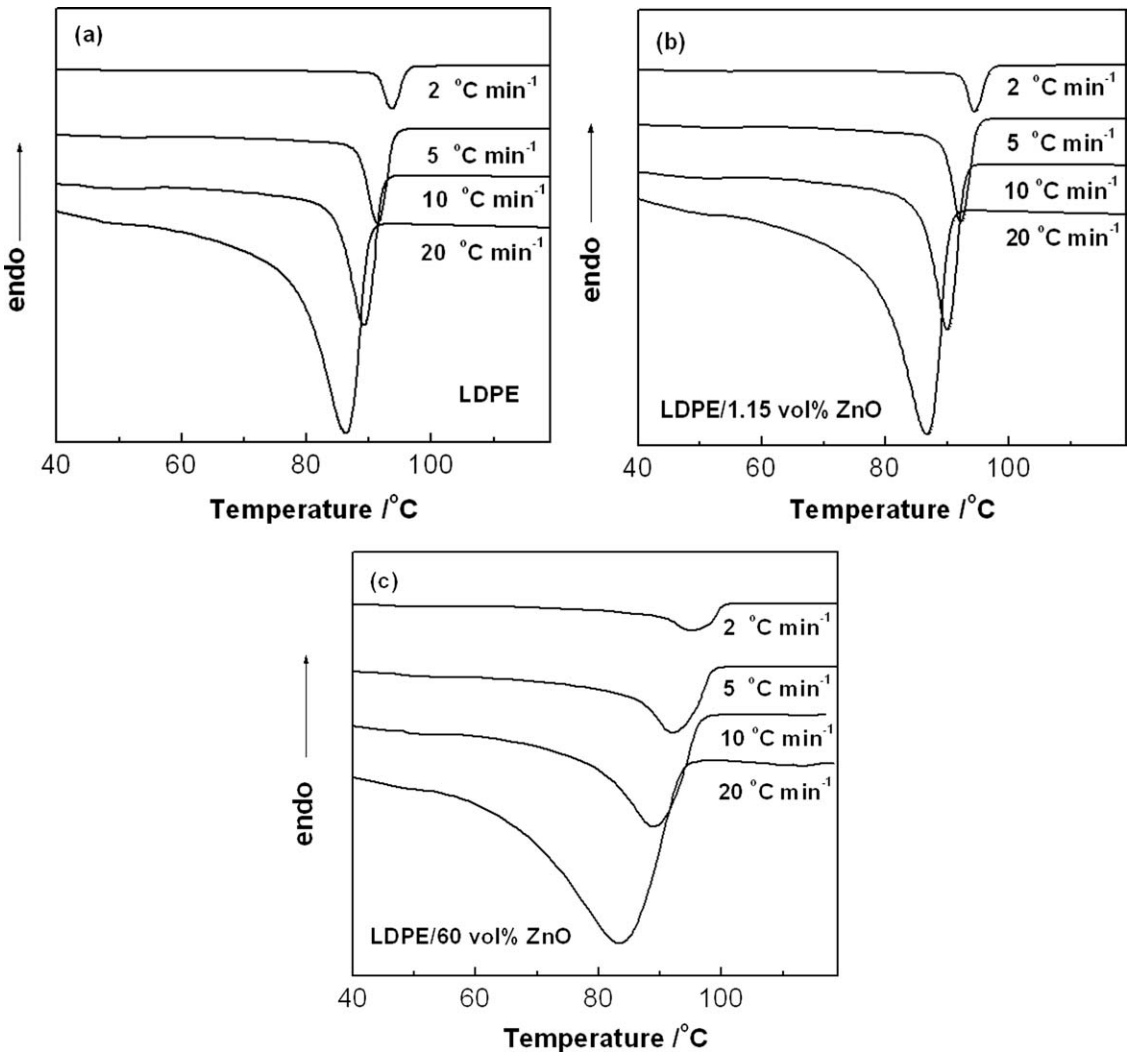

Figure 2 Nonisothermal crystallization DSC traces of pristine LDPE and its nanocomposites at various cooling rates.

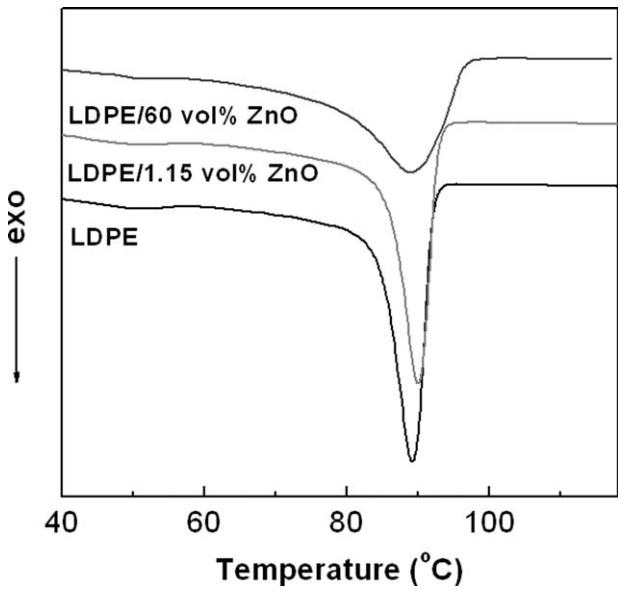

Figure 3 Comparison of DSC traces of LDPE and its nanocomposites at the cooling rate of 10°C/min.

cooling rates. For the purpose of comparison, the curves of LDPE bulk (including pristine LDPE and LDPE/1.15 vol % ZnO) are also presented. The DSC traces at cooling rate of 10°C/min for LDPE and its composites are compiled in Figure 3. A distinct exothermic peak is observed for LDPE bulk, while LDPE/60 vol % ZnO exhibits a broad peak, indicating crystallization of LDPE/60 vol % ZnO is retarded to some degree. The values of crystallization onset temperature (T_{onset}), crystallization peak temperature (T_p), and $T_{onset} - T_p$ of the samples investigated are summarized in Figure 4 and Table I. It is found that contrasting with pristine LDPE, LDPE/60 vol % ZnO possesses $\sim$ 4°C higher crystallization onset temperatures, indicating nucleation effect of ZnO on LDPE crystallization. Moreover, LDPE/60 vol % ZnO exhibits higher T_p at decreased cooling rates, while lower T_p is observed at higher cooling rates in contrast to LDPE bulk. As crystallizing at lower cooling rates, LDPE/60 vol % ZnO is kept at elevated temperatures for longer time, where

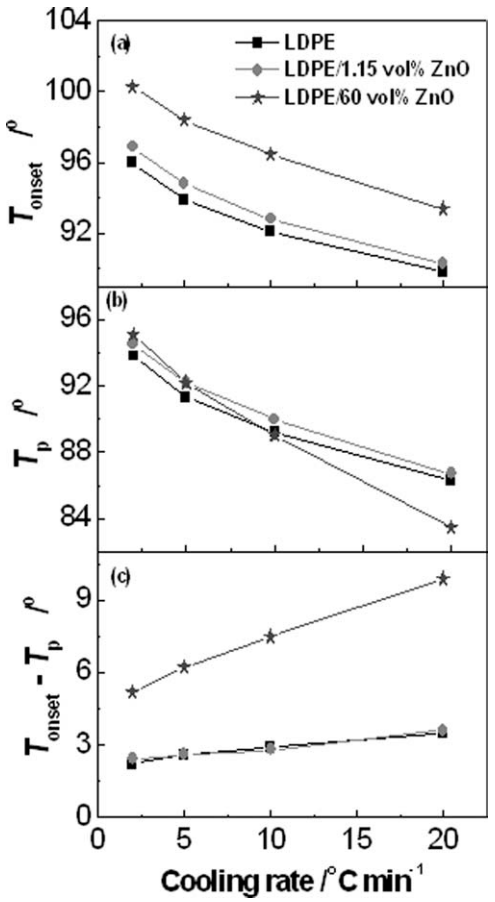

Figure 4 The values of T_{onset}, T_p, and T_{onset}—T_p of pristine LDPE and its composites at various cooling rates.

crystallization is dominated by nucleation process. Strong nucleation effect of ZnO on LDPE leads to higher T_p for LDPE/60 vol % ZnO. In contrast, LDPE/60 vol % ZnO remains at lower temperatures for longer time as crystallizing at higher cooling rates, where crystallization is controlled by crystal growth. In LDPE/60 vol % ZnO, PE crystals grow inside ZnO network, resulting in low T_p (need larger supercooling). The value of $T_{onset} - T_p$ accounts for crystallization rate to some extent. The values of $T_{onset} - T_p$ of LDPE/60 vol % ZnO are much higher than the counterpart of neat LDPE, demonstrating lower overall crystallization rate.

Crystallization temperature in Figure 2 can be transferred into crystallization time t using $t = (T_0 - T)/\phi$ (T is the temperature at crystallization time t and ϕ is the cooling rate). The relative degree of crystallinity, $X(t)$, as a function of crystallization time t is defined as:

$$X(t) = \int_0^t (dH/dt)dt / \int_0^\infty (dH/dt)dt \quad (1)$$

where t_0 and t_∞ are the initial and infinite crystallization time respectively. Plots of $X(t)$ against t are shown in Figure 5, and Figure 6 summarizes half-crystallization time ($t_{1/2}$) at various cooling rates for the samples investigated. It is found that LDPE/60 vol % ZnO shows by far larger $t_{1/2}$ value than that of LDPE bulk at each cooling rate, revealing that crystallization of the former is much slower than the latter.

Nonisothermal crystallization kinetics

Avrami equation modified by Jeziorny is used to analyze nonisothermal crystallization behavior of LDPE and its composites[37,38]:

$$1 - X(t) = \exp(-Z_t t^n) \quad (2)$$

$$\ln[-\ln(1 - X(t))] = \ln Z_t + n \ln t \quad (3)$$

where the exponent n is a mechanism constant depending on the type of nucleation and growth dimension, and Z_t is a composite rate constant relating to both nucleation and growth rate parameters. The exponent n is obtained from the slope of the straight regime of plots of $[-\ln(1 - X(t))]$ against $\ln t$ and tabulated in Figure 7 and Table I. It is found that the n values of LDPE bulk (LDPE and LDPE/

TABLE I
Nonisothermal Crystallization Parameters for Pristine LDPE and its Composites

Sample	Cooling rate (°C min^{-1})	n	T_{onset} (°C)	T_p (°C)	$t_{1/2}$ (min)	E_a (kJ mol^{-1})
LDPE	2	2.4	96.0	93.8	1.19	−343.0
	5	2.5	93.9	91.3	0.57	
	10	2.2	92.1	89.2	0.38	
	20	2.1	89.8	86.3	0.26	
LDPE/1.15 vol % ZnO	2	2.3	96.9	94.5	1.26	−330.9
	5	2.4	94.8	92.2	0.61	
	10	2.4	92.8	90.0	0.37	
	20	2.3	90.3	86.7	0.29	
LDPE/60 vol % ZnO	2	1.6	100.3	95.1	3.80	−215.7
	5	1.7	98.4	92.2	1.92	
	10	1.8	96.5	89.0	1.11	
	20	1.8	93.4	83.5	0.76	

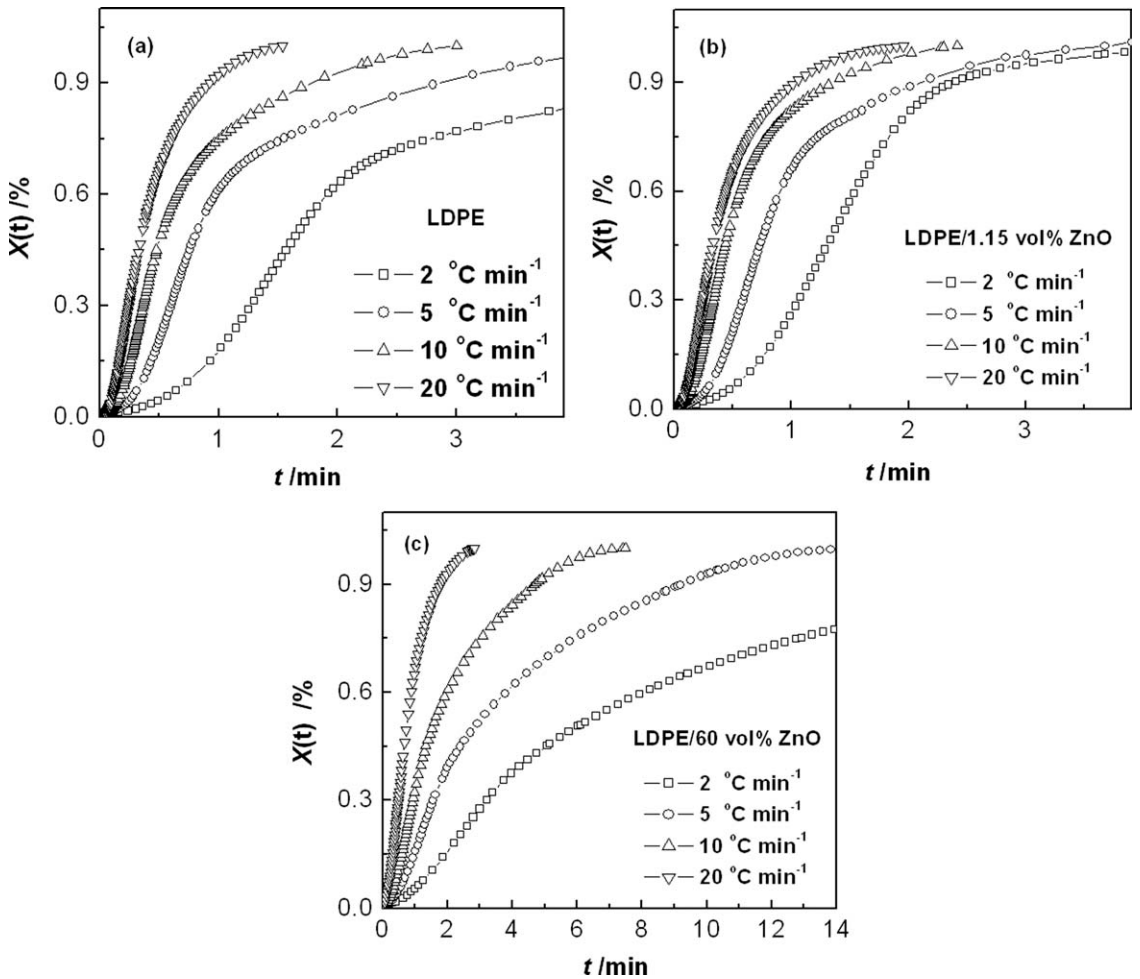

Figure 5 Plots of relative degree of crystallinity [$X(t)$] versus time (t) for LDPE and its nanocomposites at various cooling rates.

1.15 vol % ZnO) vary in range of 2.1–2.5, while a smaller n values ranging in 1.6–1.8 are observed for LDPE/60 vol % ZnO, indicating that PE crystallization in LDPE/60 vol % ZnO is confined to some extent, although it is realized that the exponent n has not same physical meaning as that in isothermal crystallization.

Assuming nonisothermal crystallization process consists of infinitesimal small isothermal crystallization steps, Ozawa deduced Avrami equation to give[39]:

$$1 - X(T) = \exp[-K(T)/\phi^m] \quad (4)$$

$$\ln[-\ln(1 - X(T))] = \ln K(T) - m \ln \phi] \quad (5)$$

where $X(T)$ is the relative degree of crystallinity at temperature T, $K(T)$ is the cooling crystallization function, and m is the Ozawa exponent and related to the mechanism of nucleation and dimension of crystal growth. If Ozawa equation is valid to describe the nonisothermal crystallization kinetics, a straight line is obtained as plotting $\ln[-\ln(1 - X(T))]$ against $\ln \phi$; however, we fail to obtain a good lineal regression.

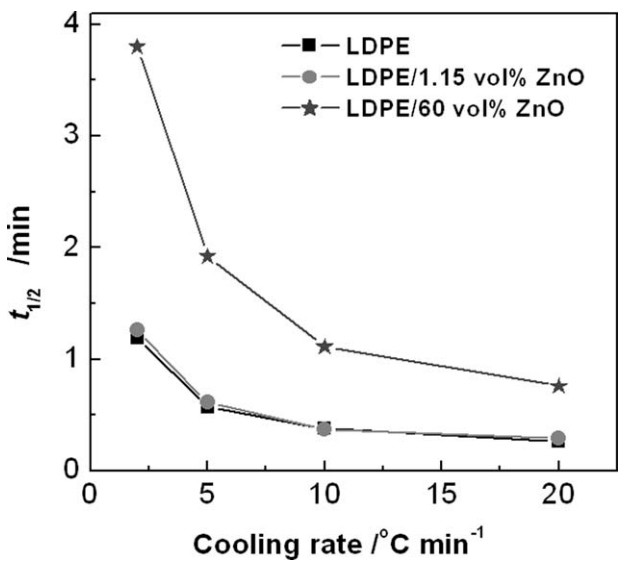

Figure 6 Comparison of crystallization half time ($t_{1/2}$) of LDPE and its nanocomposites.

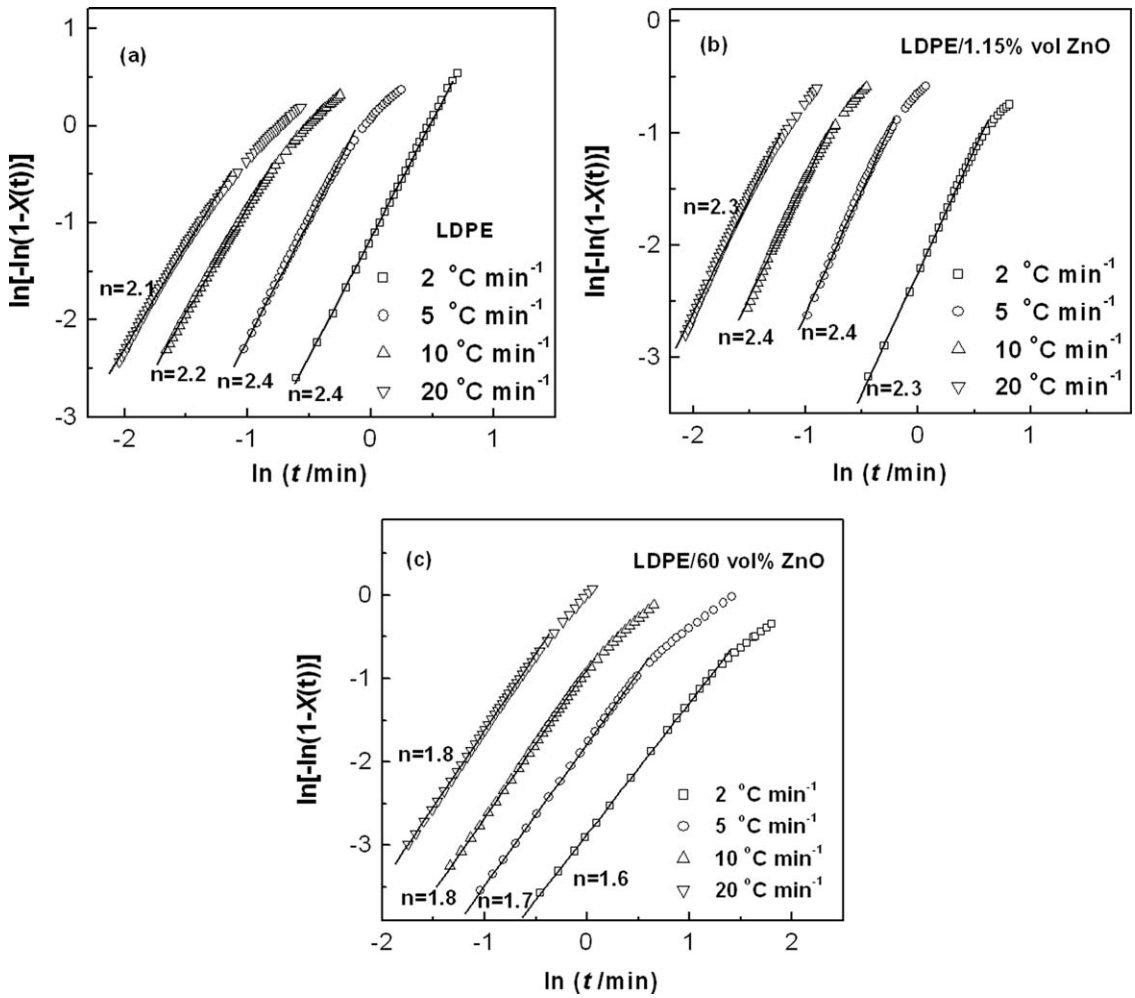

Figure 7 Plots of $\ln[-\ln(1 - X(t))]$ versus $\ln t$ for pristine LDPE and its nanocomposites.

Possible reason is that that Ozawa's theory ignores secondary crystallization, which occurs frequently at late stage of crystallization as a matter of fact.

Combing Avrami and Ozawa equations give the following equation[40]:

$$\ln \phi = \ln F(T) - \alpha \ln t \tag{6}$$

where $F(T) = [K(T)/Z_t]^{1/m}$means the necessary cooling rate at which the system reaches a certain degree of crystallinity within a unit crystallization time, and a is the ratio of Avrami exponent to Ozawa exponent (n/m). The plots of ln ϕversus ln t of LDPE and its nanocomposites are shown in Figure 8. It is apparent that a straight line is obtained for all the samples investigated. The values of $F(T)$ and a can be obtained from the intercept and slope of the straight line and summarized in Table II. It is obvious that LDPE/60 vol % ZnO has by far larger $F(T)$ than neat LDPE, showing that LDPE/60 vol % ZnO needs higher cooling rate to reach a given degree of crystallinity (larger supercooling), implying that crystallization of LDPE/60 vol % ZnO is retarded.

The activation energy of crystallization can be evaluated in terms of Kissinger method[41]:

$$\frac{d[\ln(\phi/T_p^2]}{d(1/T_p)} = -\frac{E_a}{R} \tag{7}$$

where R is the universal gas constant and E_a is the activation energy of crystallization. E_a can be obtained from the slope of plots of $\ln(\phi/T_p^2)$ versus $1/T_p$, as shown in Figure 9. The activation energy of crystallization of LDPE/60 vol % ZnO is determined to be −215.7 kJ/mol, much higher than that of LDPE (−343.0 kJ/mol). In LDPE/60 vol % ZnO, diffusion of polymer segments to crystallization sites is retarded due to geometric confinements, which leads to higher activation energy of crystallization.

Nucleation parameter

The spherulitic growth rate G of LDPE and its composites can be analyzed with Lauritzen–Hoffman equation[42]:

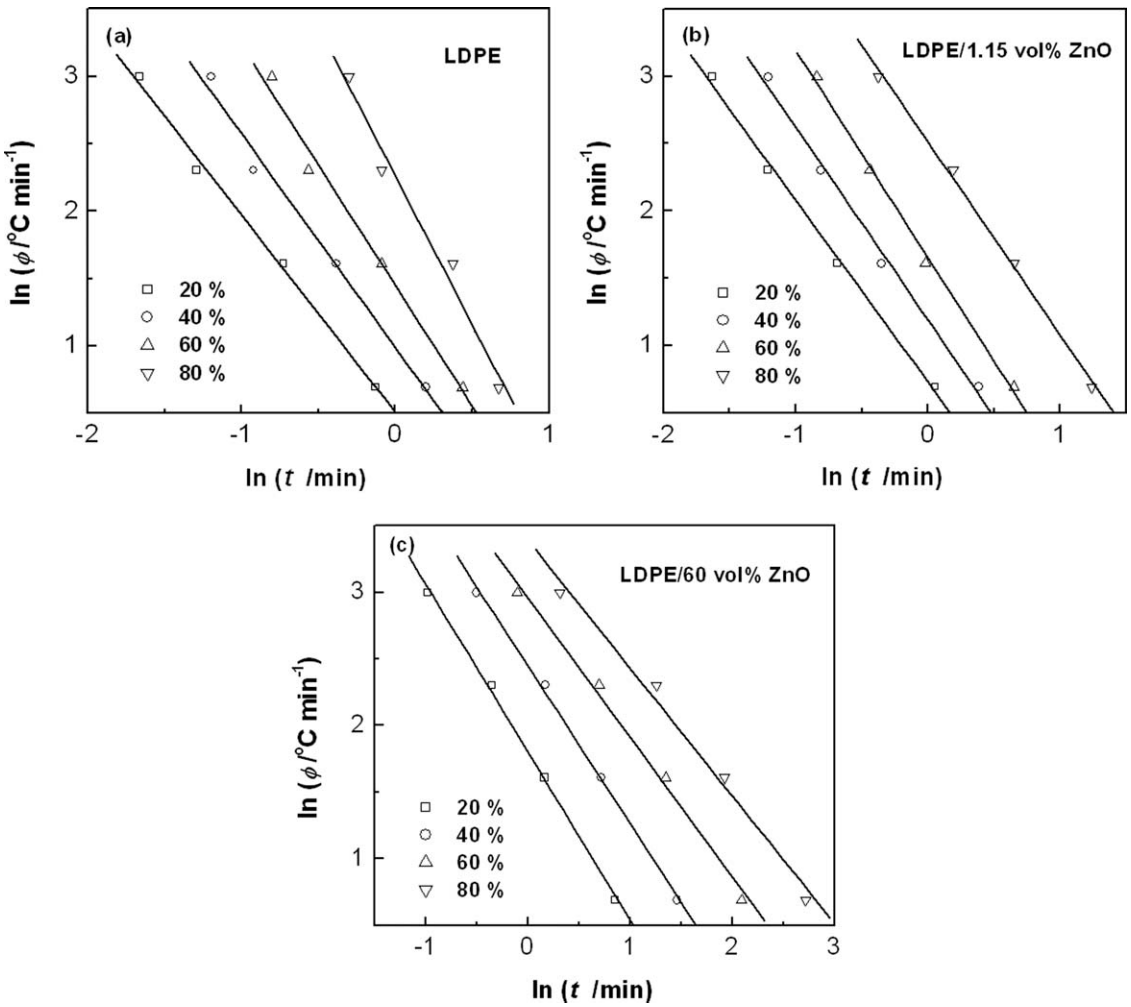

Figure 8 Plots of ln ϕ versus ln t of LDPE and its nanocomposites at various degree of crystallinity.

$$G = G_0 \exp\left(\frac{-U^*}{R(T_c - T_\infty)}\right) \exp\left(\frac{-K_g}{T_c \Delta T f}\right) \qquad (8)$$

where K_g is the nucleation parameter, T_c is the crystallization temperature, ΔT is supercooling and expressed as $T_m^0 - T_c$, f is the correction factor defined as $2T_c/(T_m^0 + T_c)$ accounting for the change in heat of fusion as the temperature is decreased below T_m^0, U^* is the activation energy for transport of macromolecular segments to the crystallization

TABLE II
***F*(*T*) and *a* for LDPE and its Nanocomposites**

Sample	$X(t)$ (%)	$F(T)$	a
LDPE	20	1.66	1.46
	40	2.68	1.59
	60	4.24	1.78
	80	9.56	2.21
LDPE/1.15 vol % ZnO	20	2.07	1.35
	40	3.28	1.43
	60	5.21	1.54
	80	12.29	1.43
LDPE/60 vol % ZnO	20	6.04	1.26
	40	11.52	1.18
	60	19.15	1.05
	80	29.51	0.96

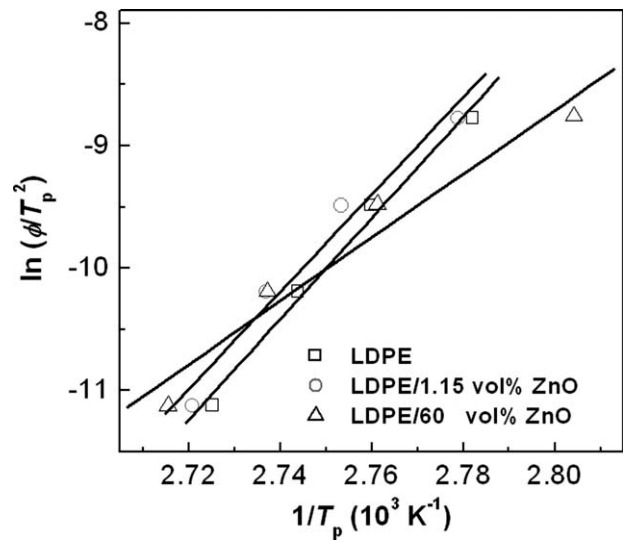

Figure 9 Plots of $\ln(\phi/T_p^2)$ versus $1/T_p$ for LDPE and its nanocomposites.

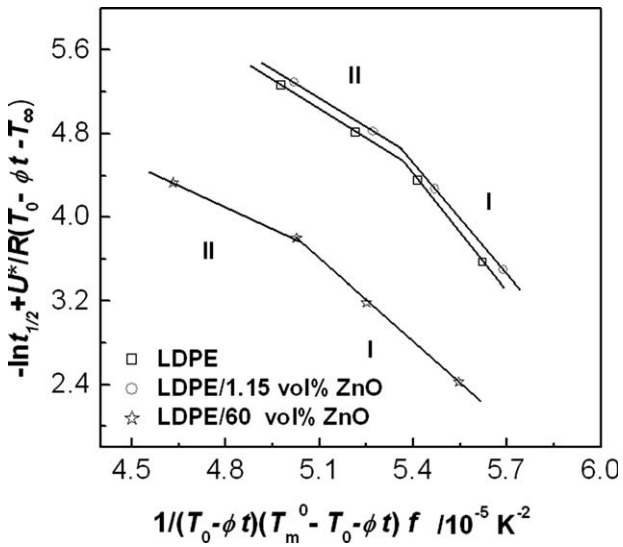

Figure 10 Plots of $-\ln t_{1/2} + U^*/R((T_0 - \phi t) - T_\infty)$ against $1/((T_0 - \phi t)(T_m^0 - (T_0 - \phi t))f$ for pristine LDPE and its nanocomposites.

site with a value of 6280 J/mol, R is the universal gas constant, T_∞^0 is the hypothetical temperature where all motion associated with viscous flow ceases, expressed as $T_g - 30$ K, being 165 K for polyethylene,[43] and G_0 is the front constant. In this equation, the first exponential accounts for the diffusion contribution to spherulitic growth rate, while the second one represents the driving force of crystallization and contains thermodynamic characteristics such as side and fold surface-free energy.

To determine the spherulitic growth rate in nonisothermal crystallization, the Lauritzen–Hoffman equation was modified by substituting crystallization temperature (T_c) with$T_0 - \phi t$ to give[44]:

$$G = G_0 \exp\left(\frac{-U^*}{R((T_0 - \phi t) - T_\infty)}\right) \times \exp\left(\frac{-K_g}{(T_0 - \phi t)(T_m^0 - (T_0 - \phi t))f}\right) \quad (9)$$

$$f = \frac{2(T_0 - \phi t)}{T_m^0 - (T_0 - \phi t)} \quad (10)$$

where T_0 is the initial crystallization temperature. The spherulitic growth rate G is regarded to be proportional to $(t_{1/2})^{-1}$, and the crystallization time $t = t_{1/2}$ is used here. When plotting $-\ln t_{1/2} + U^*/R((T_0 - \phi t) - T_\infty)$ against $1/((T_0 - \phi t)(T_m^0 - (T_0 - \phi t))f$, K_g can be determined from the slope of the lineal region, as shown in Figure 10. It is apparent from Figure 10 that all the samples investigated show crystallization regimes I and II, where the rate of deposition of secondary nuclei (i) is much smaller than the rate of the lateral surface spreading (g), and the former is comparable with the later, respectively. It is interesting that the transition temperature from regime I to regime II of LDPE/60 vol % ZnO shifts to lower temperature when compared with that of neat LDPE. Although the transition temperature, which is related to crystallization time [see eq. (9)] does not have the same meaning as that in isothermal crystallization, the lower transition temperature of LDPE/60 vol % ZnO implies that ZnO network has more pronounced effect on the formation and deposition of secondary nuclei. Possible reason is that geometric confinement of ZnO network on LDPE segments prevents LDPE from nucleating, leading to low-deposition rate of secondary nuclei and resulting lower transition temperature of LDPE/60 vol % ZnO. Similar results have been widely reported for confined crystallization of semicrystalline polymers in microdomains established by block copolymers[45] or inorganic templates.[46]

The nucleation parameter K_g is defined as:

$$K_g = \frac{nb\sigma\sigma_e T_m^0}{k\Delta H} \quad (11)$$

where k is Boltzmann constant (1.38×10^{-23} J/K), ΔH is heat of fusion per unit volume with a value of 2.80×10^8 J/m^3, T_m^0 is equivalent melting temperature (417.7 K), b is the layer thickness perpendicular to (110) reflection peak (4.11×10^{-10} m), σ is the specific free energy of lateral surfaces (11.8 erg/cm^2).[43] σ_e is the specific free energy of the folding surface. n is related to the growth mechanism of the molecular layer adsorbed on the larger surface, and the value depends on the crystallization regime, being four for regime I and III, and two for regime II. The values of K_g and σ_e of LDPE and its composites are summarized in Table III. It is found that the values of $K_g(\mathrm{I})/K_g(\mathrm{II})$ for the investigated samples

TABLE III
Values of K_g, $\sigma\sigma_e$, and σ_e for LDPE and its Nanocomposites

Sample	K_g (10^5K^2) I	K_g (10^5K^2) II	$K_g(\mathrm{I})/K_g(\mathrm{II})$	$\sigma\sigma_e$ (erg^2 cm^{-4})	σ_e (erg cm^{-2})
LDPE	3.79	1.90	2.0	2133	181
LDPE/1.15 vol % ZnO	3.57	1.86	1.9	2009	170
LDPE/60 vol % ZnO	2.64	1.34	2.0	1486	126

are ~ 2, as theoretically predicted, showing that the secondary nucleation theory can be used to analyze crystal growth of the investigated systems. LDPE/60 vol % ZnO has σ_e of 126 erg/cm^2, being 70% of neat LDPE (181 erg/cm^2). The lower σ_e of LDPE/60 vol % ZnO is likely due to the presence of ZnO around PE crystals.

CONCLUSIONS

We have investigated nonisothermal crystallization behavior of LDPE inside ZnO percolating network (LDPE/60 vol % ZnO) via DSC. The results reveal that crystallization behavior of LDPE inside ZnO percolating network is noticeably different from that of LDPE bulk (pristine LDPE and LDPE/1.15 vol % ZnO). The former shows ~ 4°C higher crystallization onset temperatures contrasting with the latter, demonstrating nucleation effect of ZnO nanoparticles on LDPE crystallization. On the other hand, much longer half-crystallization times are observed for the former, illustrating that crystallization of LDPE inside ZnO network is retarded. LDPE embedded inside ZnO network has larger crystallization activation energy and smaller specific free energy of the folding surface in contrast to neat LDPE. Nonisothermal crystallization kinetics study shows that both modified Avrami and Liu methods can be used to describe satisfactorily nonisothermal crystallization kinetics of LDPE inside ZnO network.

References

1. Muller, A. J.; Balsamo, V.; Arnal, M. L. Adv Polym Sci 2005, 190, 1.
2. Zhang, Q.; Wang, M.; Wooley, K. L. Curr Org Chem 2005, 9, 1053.
3. Liu, Y. X.; Chen, E. Q. Coord Chem Rev 2010, 254, 1011.
4. Nandan, B.; Hsu, J. Y.; Chen, H. L. Polym Rev 2006, 46, 143.
5. Castillo, R. V.; Muller, A. J. Prog Polym Sci 2009, 34, 516.
6. Wang, Y.; Rafailovich, M.; Sokolov, J.; Gersappe, D.; Araki, T.; Zou, Y.; Kilcoyne, A. D. L.; Ade, H.; Marom, G.; Lustiger, A. Phys Rev Lett 2006, 96, 028303.
7. Hamley, I. W. Adv Polym Sci 1999, 148, 113.
8. Nunez, E.; Gedde, U. W. Polymer 2005, 46, 5992.
9. Ray, S. S.; Bandyopadhyay, J.; Bousmina, M. Eur Polym J 2008, 44, 3133.
10. Liang, G. D.; Xu, J. T.; Fan, Z. Q. Eur Polym J 2007, 43, 3153.
11. Xu, J. T.; Wang, Q.; Fan, Z. Q. Eur Polym J 2005, 41, 3011.
12. Goyal, R. K.; Negi, Y. S.; Tiwari, A. N. Eur Polym J 2005, 41, 2034.
13. Xi, J. Y.; Qiu, X. P.; Zheng, S. X.; Tang, X. Z. Polymer 2005, 46, 5702.
14. Denac, M.; Musil, V.; Smit, I. J Polym Sci Polym Phys 2004, 42, 1255.
15. Perrin, F. X.; Nguyen, V.; Vernet, J. L. Polymer 2002, 43, 6159.
16. Gan, D. J.; Lu, S. Q.; Song, C. S.; Wang, Z. J. Eur Polym J 2001, 37, 1359.
17. Dufresne, A.; Kellerhals, M. B.; Witholt, B. Macromolecules 1999, 32, 7396.
18. Liang, G. D.; Xu, J. T.; Bao, S. P.; Xu, W. B. J Appl Polym Sci 2004, 91, 3974.
19. Liang, G. D.; Xu, J. T.; Wang, X. S. J Am Chem Soc 2009, 131, 5378.
20. Liang, G. D.; Tjong, S. C. Mater Chem Phys 2006, 100, 132.
21. Tjong, S. C.; Liang, G. D.; Bao, S. P. J Appl Polym Sci 2006, 102, 1436.
22. Tjong, S. C.; Liang, G. D.; Bao, S. P. Script Mater 2007, 57, 461.
23. Hedenqvist, M. S.; Backman, A.; Gallstedt, M.; Boyd, R. H.; Gedde, U. W. Compos Sci Technol 2006, 66, 2350.
24. Nan, C. W. Prog Mater Sci 1993, 37, 1.
25. Kim, S. H.; Ahn, S. H.; Hirai, T. Polymer 2003, 44, 5625.
26. Zhou, W. Y.; Duan, B.; Wang, M.; Cheung, W. L. J Appl Polym Sci 2009, 113, 4100.
27. Yu, W. X.; Zhao, Z. D.; Zheng, W. T.; Long, B. H.; Jiang, Q.; Li, G. W.; Ji, X. W. Polym Eng Sci 2009, 49, 491.
28. Wang, X. L.; Huang, F. Y.; Zhou, Y.; Wang, Y. Z. J. Macromol Sci Part B: Phys 2009, 48, 710.
29. Raka, L.; Bogoeva-Gaceva, G.; Lu, K.; Loos, J. Polymer 2009, 50, 3739.
30. Liang, G. D.; Xu, J. T.; Xu, W. B. J Appl Polym Sci 2004, 91, 3054.
31. Xu, W. B.; Liang, G. D.; Zhai, H. B.; Tang, S. P.; Hang, G. P.; Pan, W. P. Eur Polym J 2003, 39, 1467.
32. Lonkar, S. P.; Morlat-Therias, S.; Caperaa, N.; Leroux, F.; Gardette, J. L.; Singh, R. P. Polymer 2009, 50, 1505.
33. Lin, B.; Thumen, A.; Heim, H. P.; Scheel, G.; Sundararaj, U. Polym Eng Sci 2009, 49, 824.
34. Fereidoon, A.; Ahangari, M. G.; Saedodin, S. J Macromol Sci Part B: Phys 2009, 48, 25.
35. Tjong, S. C.; Liang, G. D. Mater Chem Phys 2006, 100, 1.
36. Tjong, S. C.; Liang, G. D. E-Polymers 2007, 037.
37. Avrami, M. J Chem Phys 1939, 7, 1103.
38. Jeziorny, A. Polymer 1978, 19, 1142.
39. Ozawa, T. Polymer 1971, 12, 150.
40. Liu, T. X.; Mo, Z. S.; Wang, S. E.; Zhang, H. F. Polym Eng Sci 1997, 37, 568.
41. Kissinger, H. E. J Res Natl Bur Stand 1956, 57, 217.
42. Lauritzen, J. I.; Hoffman, J. D. J Appl Phys 1973, 44, 4340.
43. Mark, J. E., Physical Properties of Polymer Handbook; American Institute of Physics: New York, 1996.
44. Lim, B. A.; McGuire, K. S.; LIoyd, D. R. Polym Eng Sci 2004, 33, 537.
45. Loo, Y. L.; Register, R. A.; Ryan, A. J.; Dee, G. T. Macromolecules 2001, 34, 8968.
46. Shin, K.; Woo, E.; Jeong, Y. G.; Kim, C.; Huh, J.; Kim, K. W. Macromolecules 2007, 40, 6617.